# Spatial variations in focused exhumation along a continental-scale strike-slip fault: The Denali fault of the eastern Alaska Range

**Jeff A. Benowitz[1], Paul W. Layer[1], Phil Armstrong[2], Stephanie E. Perry[3], Peter J. Haeussler[4], Paul G. Fitzgerald[3], and Sam VanLaningham[5]**

[1]*Geophysical Institute, University of Alaska Fairbanks, Fairbanks, Alaska 99775, USA*
[2]*Department of Geological Sciences, California State University, Fullerton, 800 N. State College Boulevard, Fullerton, California 92831, USA*
[3]*Department of Earth Sciences, Syracuse University, Syracuse, New York 13244, USA*
[4]*U.S. Geological Survey, 4200 University Drive, Anchorage, Alaska 99508, USA*
[5]*Institute of Marine Science, University of Alaska Fairbanks, Fairbanks, Alaska 99775, USA*

## ABSTRACT

**$^{40}$Ar/$^{39}$Ar, apatite fission-track, and apatite (U-Th)/He thermochronological techniques were used to determine the Neogene exhumation history of the topographically asymmetric eastern Alaska Range. Exhumation cooling ages range from ~33 Ma to ~18 Ma for $^{40}$Ar/$^{39}$Ar biotite, ~18 Ma to ~6 Ma for K-feldspar minimum closure ages, and ~15 Ma to ~1 Ma for apatite fission-track ages, and apatite (U-Th)/He cooling ages range from ~4 Ma to ~1 Ma. There has been at least ~11 km of exhumation adjacent to the north side of Denali fault during the Neogene inferred from biotite $^{40}$Ar/$^{39}$Ar thermochronology. Variations in exhumation history along and across the strike of the fault are influenced by both far-field effects and local structural irregularities. We infer deformation and rapid exhumation have been occurring in the eastern Alaska Range since at least ~22 Ma most likely related to the continued collision of the Yakutat microplate with the North American plate. The Nenana Mountain region is the late Pleistocene to Holocene (~past 1 Ma) primary locus of tectonically driven exhumation in the eastern Alaska Range, possibly related to variations in fault geometry. During the Pliocene, a marked increase in climatic instability and related global cooling is temporally correlated with an increase in exhumation rates in the eastern Alaska Range north of the Denali fault system.**

## INTRODUCTION

Regions of focused rapid (>0.5 mm/yr) exhumation are a common occurrence along major strike-slip fault systems such as the Alpine fault in New Zealand, the Denali fault in Alaska, and the San Andreas fault in California (e.g., Little et al., 2005; Fitzgerald et al., 1995; Spotila et al., 1998). However, the cause of rapid exhumation along these faults is often complex with near-field (<20 km) boundary conditions and far-field plate tectonic driving mechanisms contributing to exhumation patterns (e.g., Buscher and Spotila, 2007). Unexpectedly, the amount of exhumation along a strike-slip fault is not always a simple correlation with the degree of obliquity (of the plate motion vector with respect to the fault trace) or composition of the juxtaposed rocks (e.g., Roeske et al., 2007; Spotila et al., 2007). Climate change (Whipple, 2009), structural irregularities such as stepovers (Hilley and Arrowsmith, 2008), variations in master fault dip (Dair and Cooke, 2009), and changes in plate motion (e.g., Fitzgerald et al., 1995) all can play an important role in observed regional exhumation patterns. Given that many orogenic belts associated with strike-slip faults have heterogeneous exhumation patterns, there is a need for more case studies to examine how vertical motion is related to both near-field boundary conditions and far-field driving mechanisms (Buscher and Spotila, 2007).

The Denali fault, an active continental-scale strike-slip fault, has an asymmetric topographic signature (the Alaska Range), making the region an ideal location to examine the contribution of local and regional structures on strain partitioning and the timing of exhumation adjacent to the fault. We employ $^{40}$Ar/$^{39}$Ar, apatite fission-track (AFT), and apatite (U-Th)/He (AHe) thermochronology to document cooling, and thus exhumation patterns along the Denali fault system in the eastern Alaska Range. We find that during the Neogene, rapid exhumation in the eastern Alaska Range was initiated by the early Miocene (~22 Ma). A major contributing factor to rapid exhumation in the eastern Alaska Range during the Neogene is most likely the far-field effects of the continuing collision of the Yakutat microplate with southern Alaska (North American plate).

Our data show that exhumation is greatest in a narrow wedge (<10 km wide) proximal to the Denali fault and is partitioned across and along strike in relation to possible changes in fault geometry. Rapid ongoing exhumation in the eastern Alaska Range was possibly enhanced in the late Pliocene with the transition to more efficient glacial erosion with the onset of the Northern Hemisphere glaciation (~3 Ma; Lisiecki and Raymo, 2005) and increased erosional forcing due to climatic instability (Clift, 2010).

## GEOLOGICAL BACKGROUND

### Denali Fault

The Denali fault system in central Alaska makes a broad arc through the extensively glaciated Alaska Range (Fig. 1; St. Amand, 1957). It is a major intracontinental, right-lateral strike-slip fault that is still active as demonstrated by the 2002 M7.9 Denali fault earthquake (Eberhart-Phillips et al., 2003). Neogene movement and deformation are driven by plate tectonic processes at the Alaska southern margin subduction zone 500 km to the south (e.g., Haeussler, 2008). Matmon et al. (2006) and Mériaux et al. (2009) dated late Pleistocene moraines offset by the Denali fault in the eastern Alaska Range and show that modern slip rates are higher to the east at ~12 mm/yr, decreasing to the west at ~7 mm/yr, which suggests that slip is predominately being partitioned between the Denali fault and the Northern Foothills thrust belt and

*Geosphere*; April 2011; v. 7; no. 2; p. 455–467; doi: 10.1130/GES00589.1; 13 figures; 1 supplemental figure file; 1 supplemental text file; 5 supplemental tables.

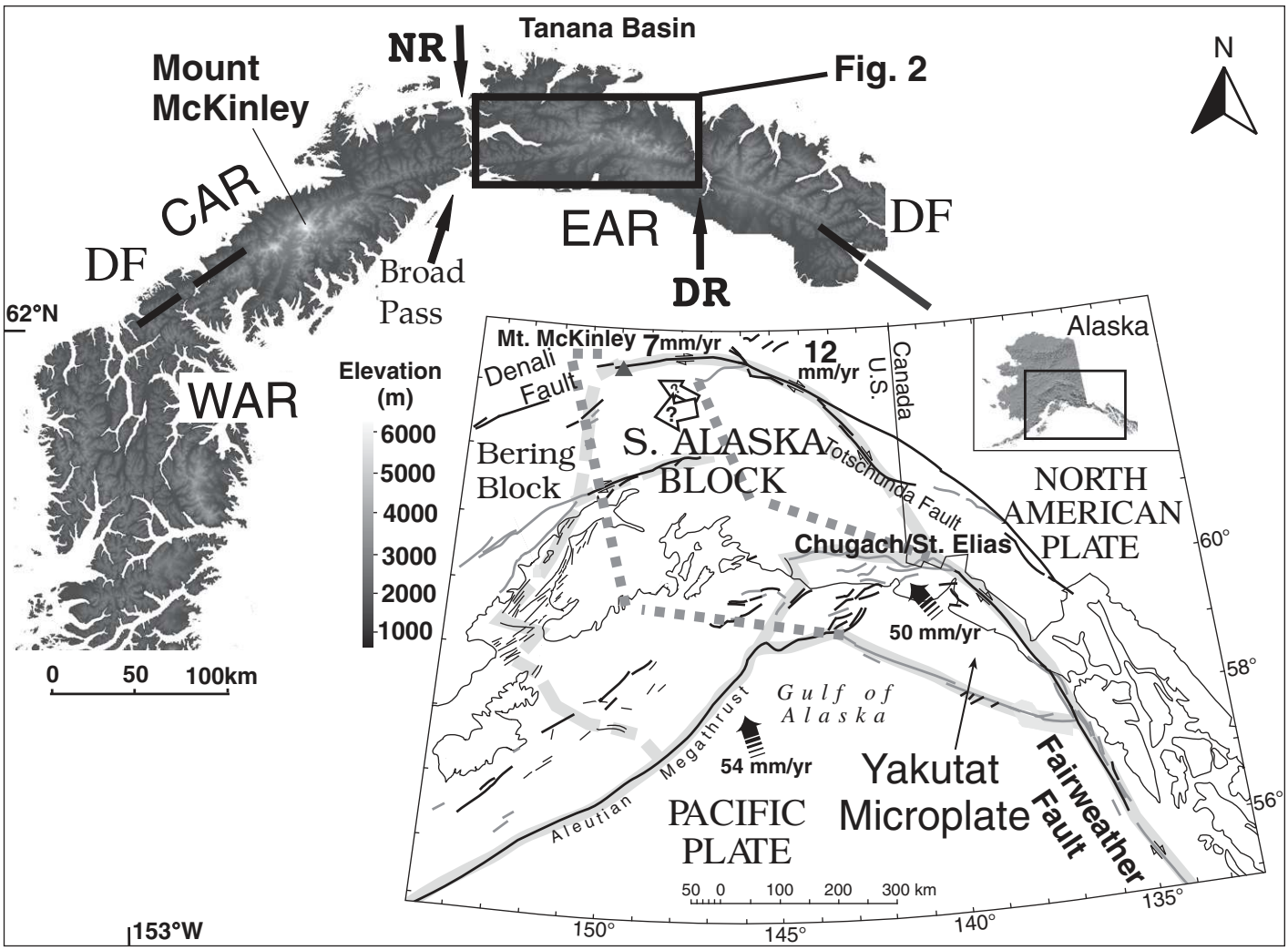


**Figure 1. Tectonic map of southern Alaska, modified from Haeussler et al. (2000), showing major faults, tectonic plates, and tectonic blocks. Decreasing westward Pleistocene Denali fault slip rates are from Matmon et al. (2006) and Mériaux et al. (2009). Yakutat– North America plate motion (solid arrow) is from Elliot et al. (2010). The open arrows show the inferred movement of the southern Alaska block with respect to North America. The western boundary of the southern Alaska block is poorly defined. The gray dashed line denotes the modern-day location of the subducted Yakutat slab beneath the continental margin (after Eberhart-Phillips et al., 2006). Detailed digital elevation model of segmented Alaska Range flooded to 1000 m elevation to emphasize higher topography. Most of the western and central Alaska Range are south of the Denali fault. The eastern Alaska Range is mostly north of the Denali fault. The rectangle delineates the study area in the eastern Alaska Range along the Denali fault shown in Figure 2.WAR—Western Alaska Range; CAR—Central Alaska Range; EAR—Eastern Alaska Range; DF—Denali Fault; DR—Delta River; NR—Nenana River.**

being siphoned off the Denali fault system onto contractional structures south of the Denali fault (Figs. 1 and 2; Bemis and Wallace, 2007; Crone et al., 2004).

### Uplift History of the Alaska Range

The ~650-km-long Alaska Range follows the curve of the Denali fault system. Areas of high-peak elevation (e.g., 6194 m in the central Alaska Range and 4216 m in the eastern Alaska Range) are separated by broad regions of low topography (e.g., Broad Pass, ~700 m, separating the central Alaska Range from the eastern Alaska Range). The majority of thermochronometric data from the Alaska Range are from the central Alaska Range (Plafker et al., 1992; Fitzgerald et al., 1993, 1995), including a 4 km vertical profile in the Mount McKinley region of the central Alaska Range (e.g., Fitzgerald et al., 1995) and from AFT work done in the western Alaska Range (Haeussler et al., 2008). These thermochronometric data sets indicate that the modern-day Alaska Range started to form ~6 Ma, although the western Alaska Range data set shows evidence of an earlier phase of rapid exhumation ~23 Ma.

With the available low-temperature data, it is logical to view the Alaska Range as a singular orogenic feature, which most likely has experienced a similar region-wide exhumation pulse at ~6 Ma. However, in the western Alaska Range and central Alaska Range, all regions of high topography (e.g., Mount McKinley) are south of the Denali fault. This observation is in stark contrast to the eastern Alaska Range

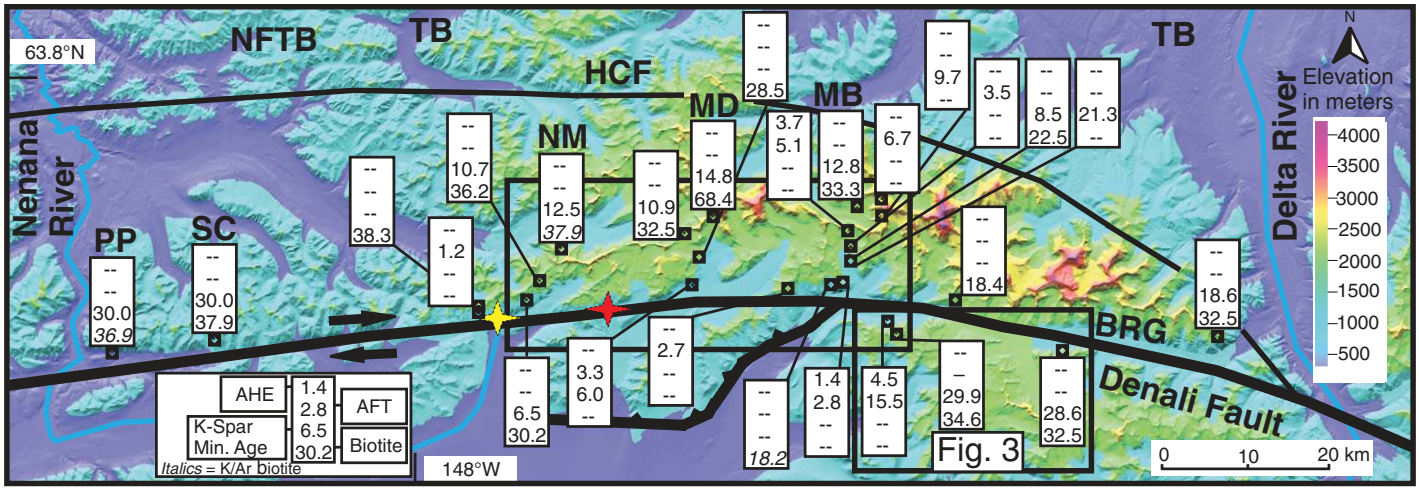


**Figure 2. Colored digital elevation map of the eastern Alaska Range showing sample locations and major faults. Sample labels show apatite helium (AHe), apatite fission-track (AFT), potassium feldspar minimum (K-spar), and biotite closure ages in descending order. Two hyphens (--) indicate no data. Italics refer to previous K-Ar work from Csejtey et al. (1992) or Nokleberg et al. (1992). The red cross shows the epicenter of the 2 November 2002 M7.9 Denali fault earthquake; the yellow cross shows the epicenter of the 23 October 2002 M6.7 Nenana Mountain earthquake. NFTB—Northern Foothills thrust belt; HCF—Hines Creek fault; SGTF—Susitna Glacier thrust fault; DF—Denali fault; PP—Panorama Peak; SC—Schist Creek pluton; NM—Nenana Mountain transect; MD—Mount Deborah transect; MB—Mount Balchen transect; BRG—Black Rapids glacier; MET—Meteor Peak region. The rectangle delineates the study area in the eastern Alaska Range along the Denali fault shown in Figure 3.**

where all of the high peaks are located north of the Denali fault (Fig. 1). In addition, Ridgway et al. (2007), in an analysis of the Miocene Usibelli Group and Pliocene Nenana Gravel within the Tanana Basin, suggested development of significant topography in the eastern Alaska Range prior to the late Miocene. Thus, the spatial and temporal evolution of the Alaska Range may be more complex than the existing data suggest.

### Physiography of the Eastern Alaska Range

Unlike the western and central Alaska Range, the high peaks of the eastern Alaska Range are sandwiched between the active McKinley strand of the Denali fault and the presumed-to-be inactive Hines Creek strand (Wahrhaftig et al., 1975). High topography (>3000 m) is limited to a narrow region (<20 km) along the north side of the Denali fault. There are numerous identified reverse and thrust faults in the greater eastern Alaska Range region with many located in the northern foothills fold and thrust belt to the north of the Hines Creek fault (Bemis and Wallace, 2007). There are few active and inactive structures identified in the ice-covered, high-peak region of the eastern Alaska Range, with the exception of the Susitna Glacier thrust fault, which was only recognized after it ruptured during the 2002 M7.9 Denali earthquake (Fig. 2; Crone et al., 2004).

Plutons north and south of the Susitna Glacier have ~70 Ma U-Pb emplacement ages (Aleinikoff et al., 2000). Nenana Mountain, Schist Creek and Panorama plutons are thought to have ~38 Ma emplacement ages based on K-Ar dating of biotite and hornblende (Csejtey et al., 1992). Both sides of the Denali fault in the high-peak region of the eastern Alaska Range experience the same climatic regime (precipitation of ~1500 to ~2000 mm/yr; Manley and Daly, 2005).

## METHODS

### Sampling and Analytical Techniques

We applied $^{40}Ar/^{39}Ar$, AFT, and AHe thermochronology to 30 bedrock samples along and across the strike of the eastern Alaska Range proximal to the Denali fault system in order to better constrain the timing and patterns of exhumation in the eastern Alaska Range. Sampling was focused along three transects north of the Denali fault: Nenana Mountain transect (NM), Mount Deborah transect (MD), and Mount Balchen transect (MB) (Fig. 2). One transect was collected south of the Denali fault in the Meteor Peak region (Fig. 3), which is the largest expanse of high topography south of the Denali fault in the eastern Alaska Range.

Eighteen samples were analyzed using $^{40}Ar/^{39}Ar$ thermochronology on potassium feldspar (K-spar) using either a laser or a resistance furnace (Supplemental Table 1[1]). Six of the furnace-run samples were then modeled using a multi-domain diffusion modeling (MDD) approach (e.g., Lovera et al., 2002) to determine thermal histories and an associated closure temperature for the minimum isochron age grouping (K-spar minimum closure age). Unaltered biotite (16), muscovite (2), and hornblende (1) (Supplemental Table 2[2]), when present, were also analyzed using $^{40}Ar/^{39}Ar$ laser step heating to supplement the time-temperature cooling trajectories of rocks in the Alaska Range.

Eight new AFT (Supplemental Table 3[3]) and three new AHe ages (Supplemental Table 4[4]) are

[1]Supplemental Table 1. Word file of $^{40}Ar/^{39}Ar$ data from potassium feldspar. If you are viewing the PDF of this paper or reading it offline, please visit http://dx.doi.org/10.1130/GES00589.S1 or the full-text article on www.gsapubs.org to view Supplemental Table 1.

[2]Supplemental Table 2. Word file of $^{40}Ar/^{39}Ar$ and K-Ar data from biotite, muscovite, and hornblende. If you are viewing the PDF of this paper or reading it offline, please visit http://dx.doi.org/10.1130/GES00589.S2 or the full-text article on www.gsapubs.org to view Supplemental Table 2.

[3]Supplemental Table 3. Word file of apatite fission-track analysis. If you are viewing the PDF of this paper or reading it offline, please visit http://dx.doi.org/10.1130/GES00589.S3 or the full-text article on www.gsapubs.org to view Supplemental Table 3.

[4]Supplemental Table 4. Word file of apatite U-Th/He data. If you are viewing the PDF of this paper or reading it offline, please visit http://dx.doi.org/10.1130/GES00589.S4 or the full-text article on www.gsapubs.org to view Supplemental Table 4.

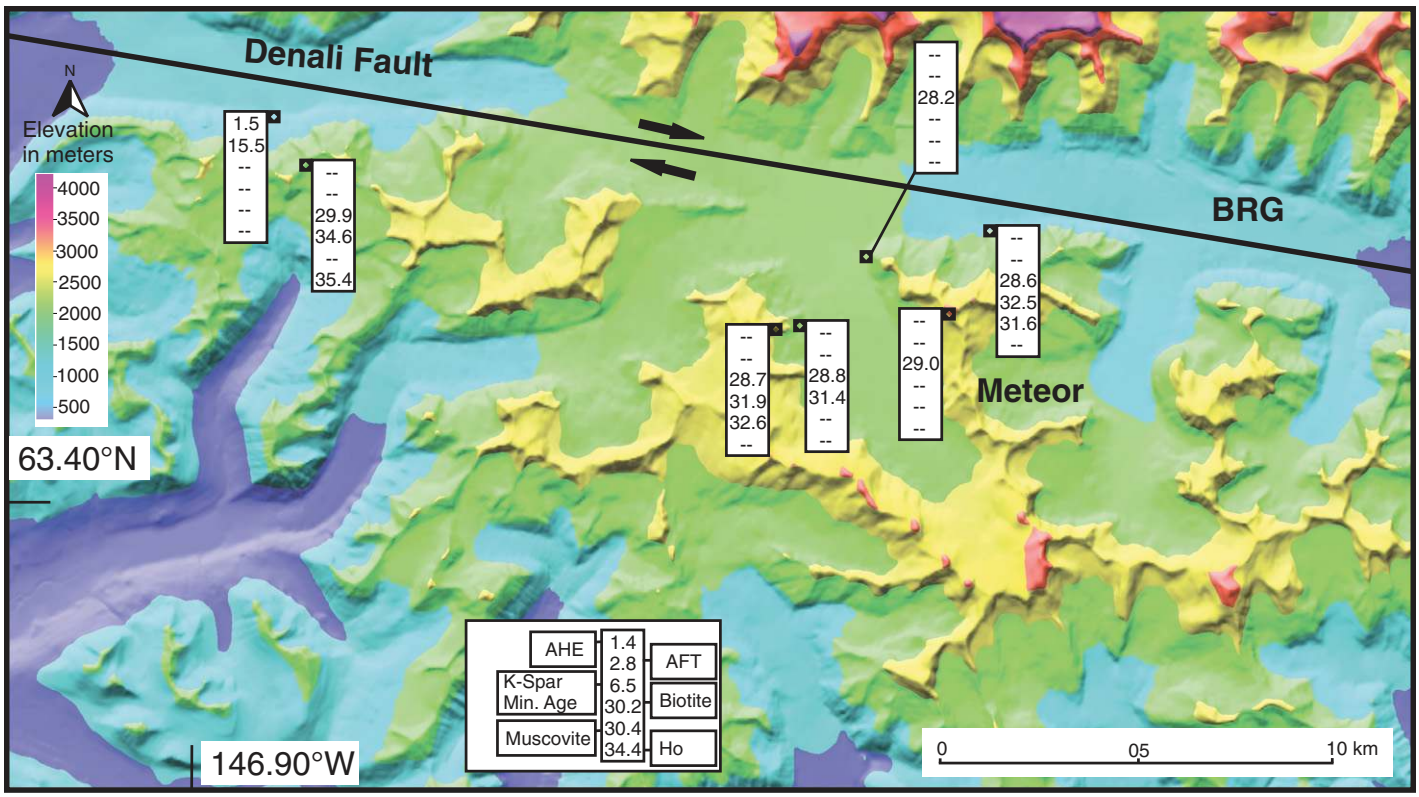


**Figure 3. Colored digital elevation map of the eastern Alaska Range showing sample locations south of the Denali fault. Sample labels show apatite helium (AHe), apatite fission-track (AFT), K-spar minimum (K-spar), biotite, muscovite, and hornblende closure ages in descending order. Two hyphens (--) refer to no data. BRG—Black Rapids glacier; Meteor—Meteor Peak region.**

presented for the eastern Alaska Range. Further details of the $^{40}Ar/^{39}Ar$, AFT, and AHe methods and closure temperature and data are presented in the Supplemental Text File[5] and Supplemental Table 5[6].

### The Geothermal Gradient and Closure Temperatures

Along the Denali fault, maximum aftershock depths of ~11 km suggest the brittle-ductile transition and approximate a regional geothermal gradient to ~30 °C/km (Fisher et al., 2004), which we use to estimate the depth to closure temperature (Tc) for the various thermochronologic systems. Approximately 30 °C/km is also the same standard regional geothermal gradient constrained by other thermochronology studies in Alaska (O'Sullivan and Currie, 1996; Haeussler et al., 2008; McAleer et al., 2009). For the purpose of constraining first-order estimates on exhumation during the Neogene, we assume that the gradient remained spatially and temporally uniform. Thus, we assume the same depth to closure isotherms across the region. We acknowledge that for the low-temperature AFT and AHe data, due to their lower closure temperatures, and hence shallower depths of closure, plus higher Pliocene–Quaternary exhumation rates, this assumption is a simplification and the resulting trends, an approximation. However, the majority of the data in this manuscript are from high-temperature thermochronometers with deep closure depths. These ages are less affected by high Quaternary exhumation rates and variation in isotherm depth related to surface topography (e.g., Braun et al., 2006). We first discern whether the higher temperature cooling ages are related to initial emplacement cooling or cooling related to exhumation before calculating depth of closure.

We use standard closure temperatures for $^{40}Ar/^{39}Ar$ dating of hornblende (550 °C), muscovite (Tc 400 °C), biotite (Tc 350 °C), K-spar (Tc 150 °C), and also for AFT (Tc 110 °C) and AHe (Tc 65 °C) cooling ages (Harrison et al., 2009; Reiners and Ehlers, 2005; e.g., McDougall and Harrison, 1999). Precise spatial differences in exhumation rates and/or trends are not critical because the variations are large enough to be significant and are not artifacts of variations in geothermal gradients. We also do not give quantitative rates of cooling, but instead discuss overall trends in cooling rates to avoid over interpreting time-averaged thermochronological constraints. In addition, the dip of the Denali fault at depth is poorly constrained (see discussion below), but we assume general subvertical rock trajectories based on available structural work done in the region (Sherwood and Craddock, 1979). These assumptions about temperature and, hence, depth of closure allow us to examine near-field exhumation trends and patterns during the Neogene in the eastern Alaska Range.

## RESULTS

Most hornblende, muscovite, and biotite analyses from samples on both sides of the Denali fault show well-defined $^{40}Ar/^{39}Ar$ age

[5]Supplemental Text File. PDF file of supplemental text. If you are viewing the PDF of this paper or reading it offline, please visit http://dx.doi.org/10.1130/GES00589.S5 or the full-text article on www.gsapubs.org to view the Supplemental Text File.

[6]Supplemental Table 5. Word file of $^{40}Ar/^{39}Ar$ data for biotite, muscovite, hornblende, and K-spar. If you are viewing the PDF of this paper or reading it offline, please visit http://dx.doi.org/10.1130/GES00589.S6 or the full-text article on www.gsapubs.org to view Supplemental Table 5.

plateaus with simple spectra with little or no argon loss (Figs. A1 to A19 in the Supplemental Figure File[7], Supplemental Tables 2 and 5 [see footnotes 2 and 6]). This evidence of unaltered samples is demonstrated by the high concordance between integrated ages (whole gas) and plateau ages for the hornblende, muscovite, and biotite analyses (Fig. 4).

Along the Balchen transect, biotite cooling ages decrease southwards toward the Denali fault from ~33.3 Ma to ~18.4 Ma (Fig. 2). Proximal Black Rapids, Mount Deborah, and the far southeastern part of Nenana Mountain pluton have biotite cooling ages of ~32 Ma to ~18 Ma. The west part of the Nenana Mountain region, Schist Creek, and Panorama plutons have biotite ages of ~38 Ma. The Mount Deborah sample, which is most distal from the Denali fault, has a biotite age of ~68 Ma.

K-spar minimum closure ages for Nenana Mountain, Mount Deborah, Mount Balchen, and the north side of the Black Rapids glacier regions range from ~18.6 Ma to ~6.0 Ma. K-spar minimum closure ages west of the Nenana Mountain region and also south of the Denali fault (Figs. 2 and 3) are distinctly older (~28.6 to ~30.8 Ma). K-spar MDD modeling of six samples from the region north of the Denali fault indicates that K-spar minimum ages represent cooling through the ~150 °C isotherm. We interpret MDD models as indicating a diffuse pattern for the initiation of rapid cooling.

Approaching the Denali fault from the north, AFT ages generally decrease from ~6.7 Ma to ~1.2 Ma with the youngest ages in the Nenana Mountain region. AHe ages north of the Denali fault range from ~4.0 Ma to ~1.5 Ma. Near the south side of the Denali fault, we report an AFT age of ~15.5 Ma and one AHe age of ~4.5 Ma (Figs. 2 and 3).

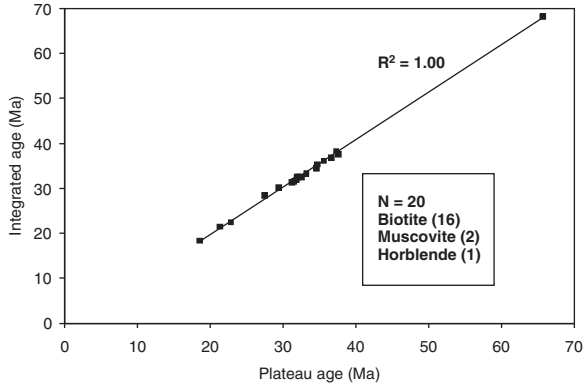


**Figure 4. Integrated age versus plateau age for the entire $^{40}Ar/^{39}Ar$ hornblende, muscovite, and biotite data set. The similarity between the two age determinations demonstrates little or no argon loss for the sample analyses.**

## DISCUSSION

### Along-Strike Exhumation

#### *North of the Denali Fault*

Biotite ages of samples from the westernmost Nenana Mountain region have ages (~38.3 Ma to ~36.2 Ma; Fig. 2) concordant with the emplacement age of the pluton (~38 Ma) indicating postemplacement rapid cooling and not exhumation-related cooling. Schist Creek and Panorama plutons have biotite ages of ~38 Ma and are interpreted as being related to initial melt emplacement cooling as well.

Biotite ages of ~32 Ma to ~18 Ma from intrusions on the north side of the Black Rapids glacier and eastern edge of the Nenana Mountain pluton are interpreted as exhumation-related cooling ages based on the respective emplacement ages of the plutons (~70 Ma; ~38 Ma). Because the emplacement age of the Balchen intrusion is ~70 Ma (Aleinikoff et al., 2000), the trend of younger biotite ages (~33.3 Ma to ~18.4 Ma) toward the Denali fault demonstrates that the biotite ages are cooling ages related to exhumation, with exhumation increasing toward the fault (Fig. 2). The Mount Deborah pluton, like the Balchen pluton, is assumed to have an ~70 Ma emplacement age based on the upper sample having a biotite age of ~68.4 Ma (Fig. 2). The Mount Deborah samples (proximal to the Denali fault) have biotite cooling ages that are related to exhumation (~32 Ma to ~28 Ma).

The K-spar minimum ages (~30 Ma), the flat shape of the K-spar $^{40}Ar/^{39}Ar$ age spectra, and biotite $^{40}Ar/^{39}Ar$ ages (~38 Ma) for the Panorama and Schist Creek plutons imply rapid postemplacement cooling for both plutons through the minimum closure temperature for K-spar (Figs. 5 and 6). The downward-stepping K-spar $^{40}Ar/^{39}Ar$ age spectra and MDD modeling of furnace runs of samples from Nenana Mountain, Mount Deborah, Mount Balchen transects, and the Black Rapids glacier regions north of the Denali fault confirm that the minimum closure ages indicate rapid cooling due to exhumation through ~150 °C (Figs. 5, 7, and 8).

The MDD K-spar thermal models from north of the Denali fault show relatively diverse cooling histories with rapid cooling occurring in individual samples between ~22 Ma and ~6 Ma (Fig. 8). These north-side thermal models suggest heterogeneous exhumation along and across the strike of the Denali fault. AFT ages range from ~6.7 Ma (Mount Balchen) to ~1.2 Ma (Nenana Mountain region), and AHe ages range from ~4 Ma to ~1.5 Ma (Mount Balchen). Combined with the biotite and K-spar data, the AFT and AHe ages indicate that Neogene rapid exhumation has been a long-term (~22 Ma to present) phenomenon along the north side of the Denali fault in the eastern Alaska Range.

#### *South of the Denali Fault*

In contrast to samples north of the fault, orthogneiss samples south of the Denali fault have flat, ~30 Ma K-spar age spectra that are concordant with $^{40}Ar/^{39}Ar$ hornblende, muscovite, and biotite ages (~35 Ma to ~31 Ma) from the same samples (Figs. 5 and 9). We interpret this rapid cooling event as a short-lived metamorphic event because the samples have a penetrative fabric, and they have concordant $^{40}Ar/^{39}Ar$ cooling ages, which is in general agreement with past interpretations for the region (e.g., Nokleberg et al., 1992). Proximal to the Denali fault, ~15.5 Ma AFT and ~4.5 Ma AHe ages on the south side of the fault are older than AFT ~1.2 Ma AFT and ~1.5 Ma AHe ages on the north side of the fault. These low-temperature data combined with the aforementioned $^{40}Ar/^{39}Ar$ thermochronology results indicate a different exhumation history for the south side of the Denali fault than the north side.

### Across-Strike Influence of the Denali Fault

The trend of cooling ages decreasing toward the Denali fault from the north is directly correlated with both elevation (Fig. 10A) and distance from the fault (Fig. 10B) for all four thermochronometric systems. This relationship indicates that exhumation just north of the Denali fault in the eastern Alaska Range has been focused there and persisted for at least the past ~20 m.y. Although cooling age is correlated with both elevation and distance from the Denali fault, distance from the fault is more significant. A good example of this relationship is seen in the Mount Balchen transect K-spar minimum cooling age data where proximity to the Denali fault has a stronger effect on cooling age than elevation (Fig. 10).

[7]Supplemental Figure File. PDF file of 43 images. If you are viewing the PDF of this paper or reading it offline, please visit http://dx.doi.org/10.1130/GES00589.S7 or the full-text article on www.gsapubs.org to view the Supplemental Figure File.

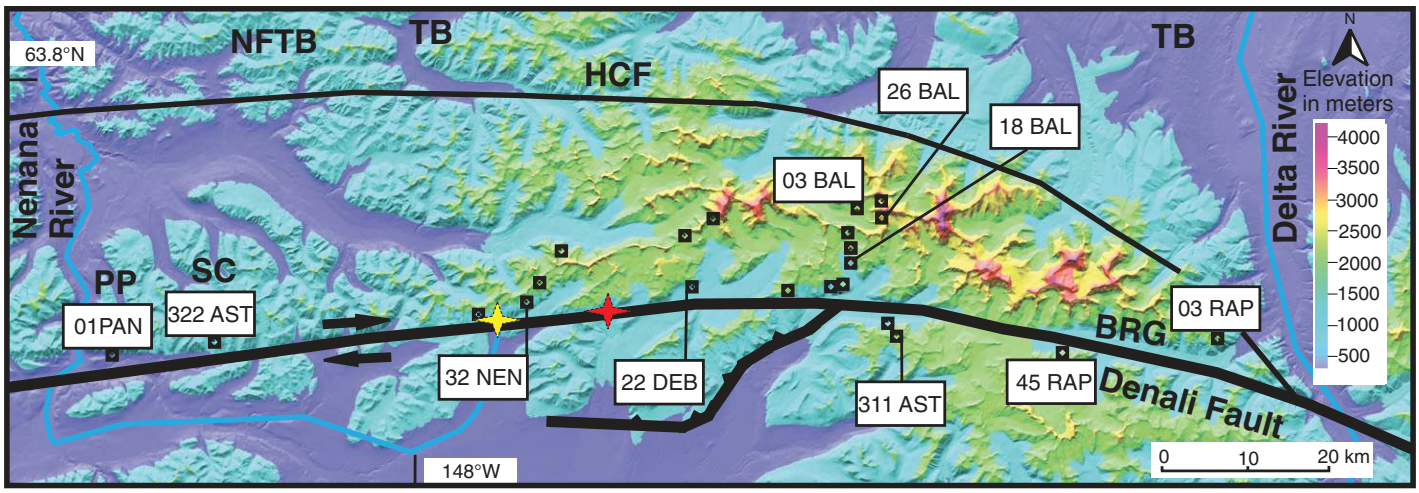


**Figure 5. Colored digital elevation map of the eastern Alaska Range showing major faults and sample locations for those in Figures 6, 7, 8, and 9. The red cross shows the epicenter of the 2 November 2002 M7.9 Denali fault earthquake; the yellow cross indicates the epicenter of the 23 October 2002 M6.7 Nenana Mountain earthquake. NFTB—Northern Foothills thrust belt; HCF—Hines Creek fault; SGTF—Susitna Glacier thrust fault (shown in blue); PP—Panorama Peak; SC—Schist Creek pluton; BRG—Black Rapids glacier.**

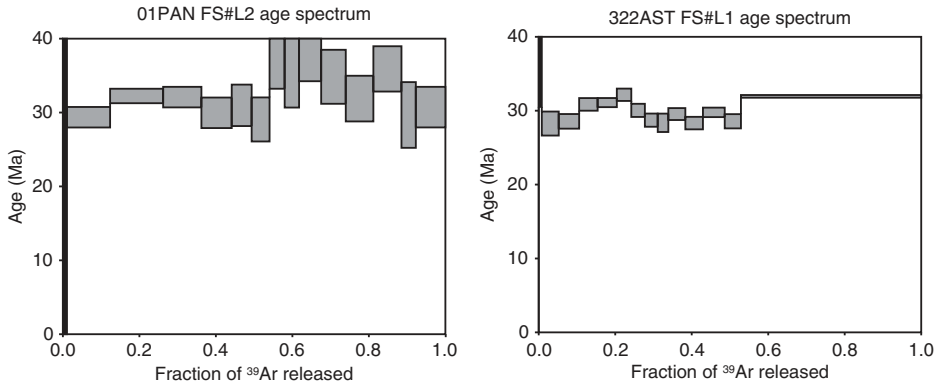


**Figure 6. $^{40}Ar/^{39}Ar$ age spectra for K-spar from sample 01PAN from Mount Panorama and sample 322AST from Schist Creek pluton. The general flat shape of the age spectra implies rapid postemplacement cooling. Sample locations are shown on Figure 5.**

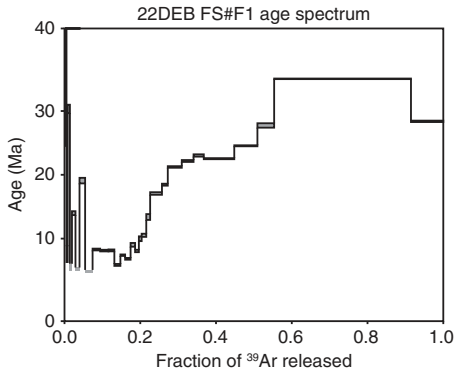


**Figure 7. $^{40}Ar/^{39}Ar$ age spectra for K-spar from sample 22DEB from the Mount Deborah transect. The downstepping nature of the release indicates a prolonged and complicated thermal history. Sample location is shown on Figure 5. See Figs. A22–A31 in the Supplemental Figure File (see footnote 7) for other samples.**

Thermochronometric data from the south side of the Denali fault show no strong elevation or distance-from-fault trends. Muscovite, biotite, and K-spar minimum cooling ages are all concordant and suggest very rapid cooling at ~30 Ma throughout the area (Figs. 2 and 3). No graphical representation is presented because the cooling ages would simply overlap—biotite ages are all ~31 Ma; K-spar minimum ages are all ~29 Ma.

### Overall Depth of Exhumation Patterns in the Eastern Alaska Range

In the eastern Alaska Range, the depth of Neogene exhumation varies dramatically across and along the Denali fault allowing for general contouring of Neogene minimum or maximum exhumation depths (Fig. 11). The difference in cooling ages across the Denali fault defines a narrow (<~10km) wedge of deep Neogene exhumation in the eastern Alaska Range. It is also clear that the region south of the Denali fault in the eastern Alaska Range experienced less total exhumation during the Neogene than the region juxtaposed to the north.

Samples south of the Denali fault have only been exhumed through the AFT closure system during the Neogene and experienced less than ~5 km of exhumation since ~28 Ma based on the assumed geothermal gradient of ~30 °C/km, the assumed Tc of ~150 °C for K-spar, and the concordant muscovite, biotite, and K-spar ages in the region. To the west, Panorama and Schist Creek plutons experienced less than ~5 km of exhumation based on the $^{40}Ar/^{39}Ar$ biotite and $^{40}Ar/^{39}Ar$ K-spar systems being concordant. Because $^{40}Ar/^{39}Ar$ biotite ages (Tc ~350 °C) from samples north of the Denali fault between the Black Rapids glacier and the southeast end of the Nenana Mountain pluton are exhumation-related closure ages, this region experienced significant enough unroofing to exhume rocks that have passed through the ~350 °C isotherm. Therefore, the region has undergone a minimum of ~11 km of exhumation. The region around the epicenter of the 23 October 2002 M6.7 Nenana Mountain earthquake has experienced at least ~5 km of exhumation. This conclusion

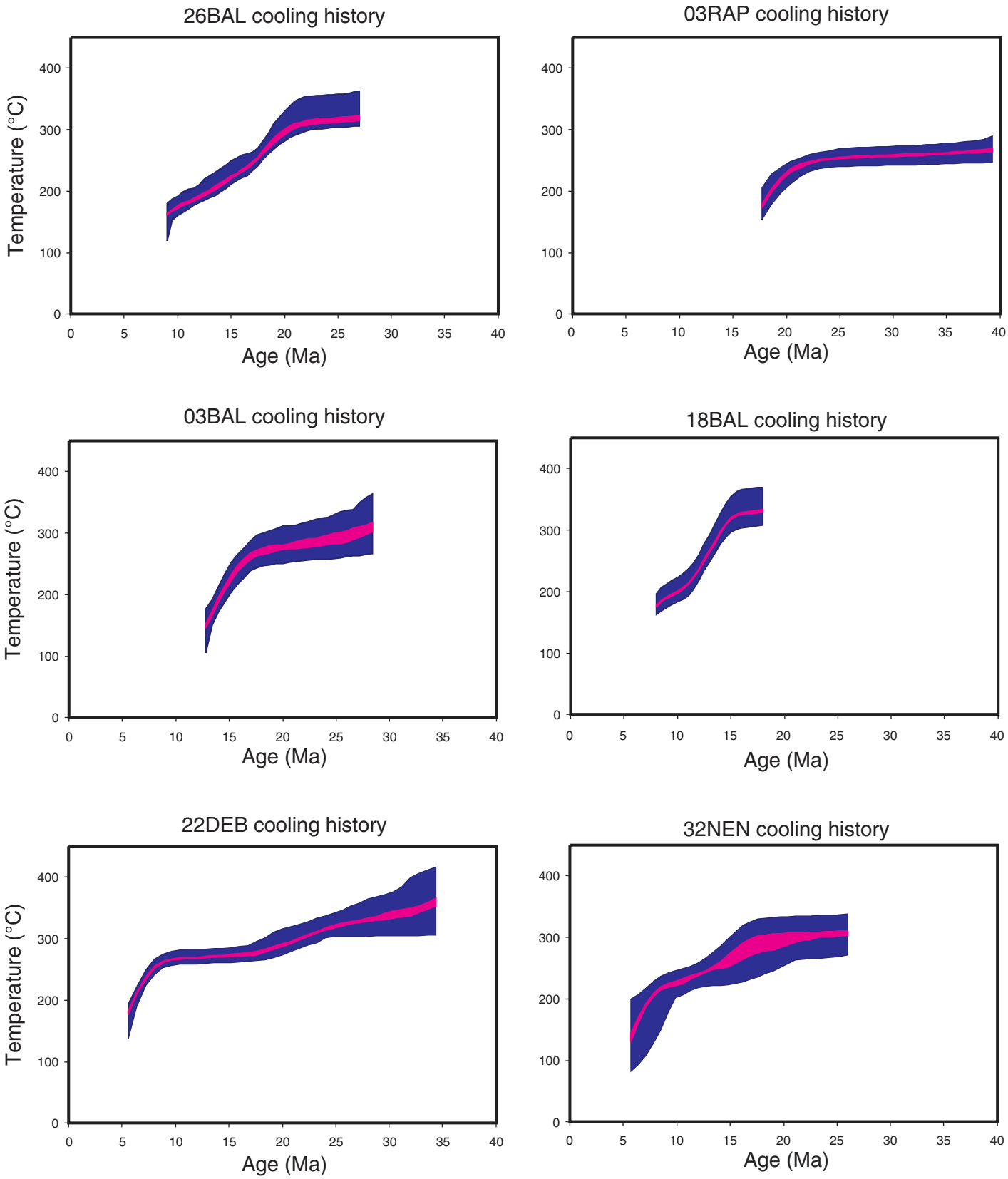


**Figure 8. Monotonic multiple diffusion domain (MDD) thermal models for K-spar from samples 26BAL, 03RAP, 03BAL, 18BAL, 22DEB, and 32NEN. The MDD magenta band is the 90% confidence interval of the mean, and the purple band is the 90% confidence of the distribution. Sample locations are shown on Figures 5.**

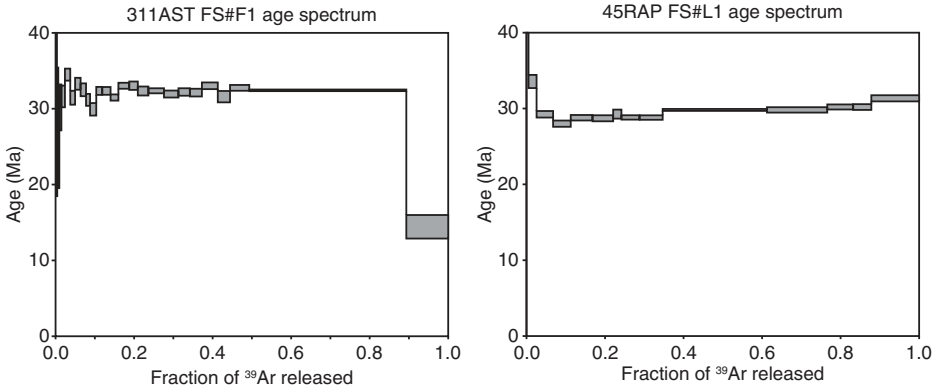


**Figure 9. $^{40}Ar/^{39}Ar$ age spectra for K-spar for samples 311AST and 45RAP from south of the Denali fault. The flat shape of the age spectra implies rapid cooling, which we interpret as a short-lived metamorphic event based on rock fabric. Sample locations are shown on Figure 5.**

is based on K-spar minimum ages being exhumation-related closure ages, but the $^{40}Ar/^{39}Ar$ biotite ages of these samples are concordant with the emplacement age of the pluton. This relationship puts limits on the possible depth of exhumation for these samples at a maximum of ~11 km. The Nenana Mountain region is located at the western end of the high topography in the eastern Alaska Range, where we found the youngest AFT age (1.2 Ma) and where young cooling ages transition to older cooling ages farther to the west (Fig. 2).

Modern earthquake behavior also varies along strike. The 23 October 2002 M6.7 Nenana Mountain earthquake had a westward-propagating rupture (Lu et al., 2003). However, the 2002 7.9M Denali fault earthquake had an eastward-propagating surface rupture (Eberhart-Phillips et. al., 2003) implying a possible change in the fault behavior from east to west along the fault (Ratchkovski et al., 2004) in the Nenana Mountain region. This is the same region where we see young AFT cooling ages in samples that have not been exhumed deeply enough to have exhumation-related biotite closure ages (Figs. 2 and 11) suggesting a possible Pleistocene increase in exhumation rates in the area.

### Role of Denali Fault Dip in Driving Exhumation

Strike-slip faults by definition involve predominately lateral slip, along a vertical to high-angle fault plane (e.g., Sylvester, 1988). Asymmetric basin development as seen in the North Anatolian fault (Cormier et al., 2006) and

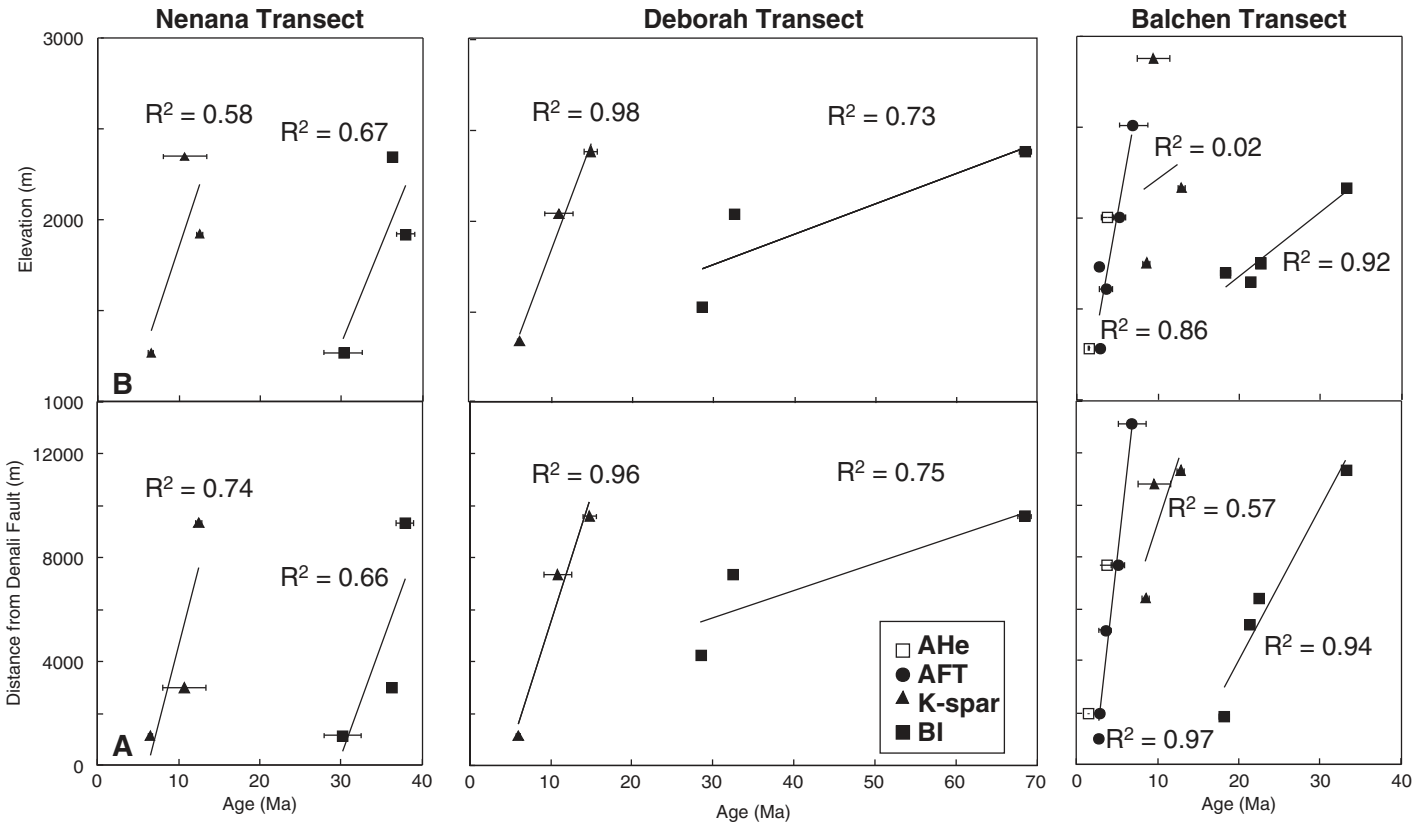


**Figure 10. Exhumation cooling ages versus (A) distance from the Denali fault and (B) elevation above sea level for all samples from the three transects shown in Figure 2. The Denali fault is interpreted as lying in the center of each glacier in the study area. Lines show best linear fit to data points of same thermochronology method. Correlation coefficient is shown next to the best-fit lines. Because there were only two AHe samples from near Mount Balchen, these AHe ages are shown without a trend line. Although cooling age in all systems is overall correlated with both elevation and distance from the Denali fault, distance from the fault is more significant. A good example of this relationship is seen in the Mount Balchen transect K-spar minimum age data where proximity to the Denali fault has a stronger effect on cooling age than elevation.**

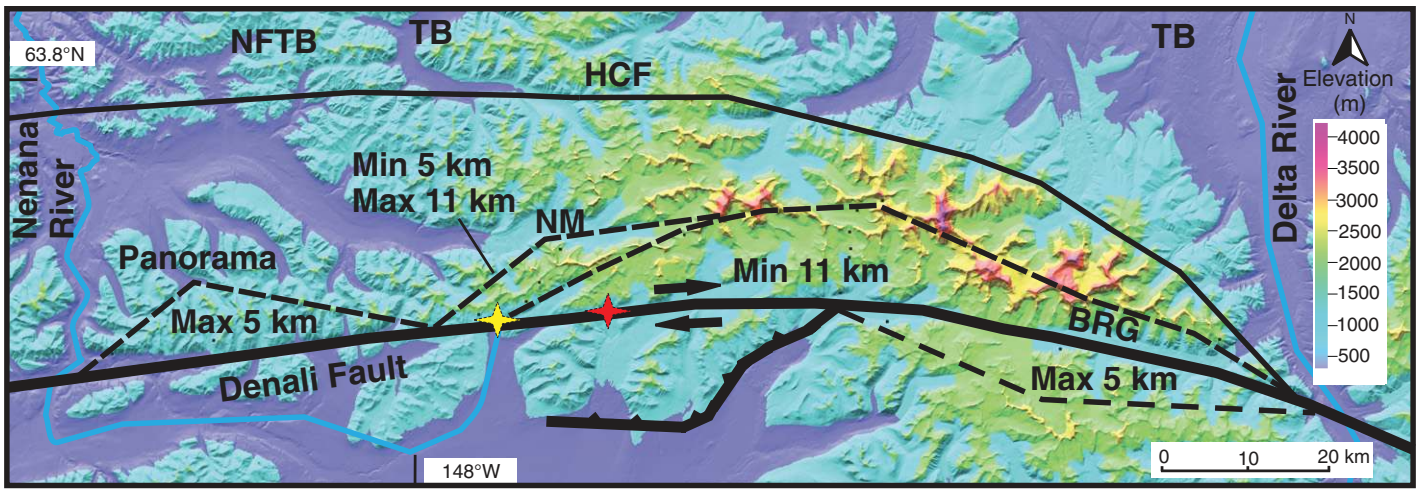


**Figure 11. Regions (contours) of varying exhumation depth along the Denali fault based on the current set of high temperature hornblende, muscovite, biotite, and K-spar minimum closure ages. The red cross shows the epicenter of the 2 November 2002 M7.9 Denali fault earthquake; the yellow cross indicates the epicenter of the 23 October 2002 M6.7 Nenana Mountain earthquake. NFTB—Northern Foothills thrust belt; HCF—Hines Creek fault; SGTF—Susitna Glacier thrust fault; BRG—Black Rapids glacier region; NM—Nenana Mountain region; Panorama—Panorama and Schist Creek plutons. The current locus of rapid exhumation is inferred to be near the epicenter (yellow cross) of the 23 October 2002 M6.7 Nenana Mountain earthquake and related to the edge of a segment of north-dipping fault plane.**

variations in uplift rates along the San Andreas fault (Dair and Cooke, 2009) have recently been explained through models involving nonvertical fault planes. Variations in fault dip (both along strike and at depth) have been thoroughly documented for the Alpine fault of New Zealand (e.g., Little et al., 2005) and may be applicable to many strike-slip fault systems.

The dip of the Denali fault is near vertical along the Delta River corridor where the topography is low (Fisher et al., 2004). The measured surface dip of the Denali fault is ~80° N in the region between the Balchen and Deborah transects (Haeussler et al., 2004), but it is not well constrained beneath the glaciers or at depth. If the dip of the Denali fault plane (Fig. 12) varies along strike (east to west) from north dipping in parts of the eastern Alaska Range (Fig. 12C), to near-vertical (Fig. 12B) in areas of low elevation like Broad Pass, to south dipping in the central Alaska Range (Fig. 12A), then the change in fault geometry may partially or fully explain the variations in along- and across-strike variations in topography.

An alternative explanation for the high topography and/or deep exhumation north of the Denali fault in the eastern Alaska Range is the fact that there may be unmapped, ice-covered structures, splaying off the eastern Denali fault system that are the results of partitioned strain. The along-strike (west to east) change from deep exhumation to shallow exhumation west of the Nenana Mountain transect occurs along a section of the Denali fault that is straight. This relationship indicates that variations in obliquity of convergence are most likely not driving exhumation patterns in the eastern Alaska Range.

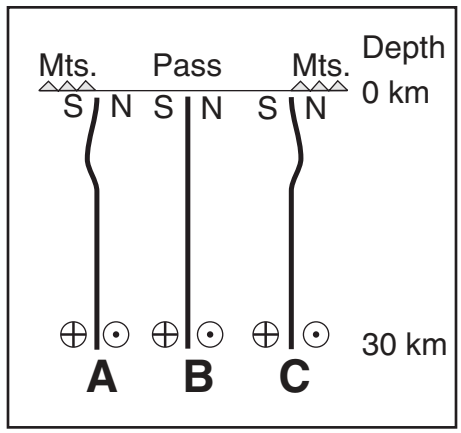


**Figure 12. Schematic model of variations in the dip of the Denali fault plane, at depth, which may contribute to asymmetric topographic development along the Denali fault. View is along the fault plane looking westward. Note, the Denali fault in the central Alaska Range may dip south (A), the broad pass region may be vertical (B), and the Denali fault in the eastern Alaska Range may dip to the north (C), resulting in asymmetric topographic development.**

### Climate and Exhumation Rate Trends in the Eastern Alaska Range

The increase in exhumation rates has been shown to correlate with climate change in tectonically active regions of Alaska (e.g., Berger et al., 2008a; McAleer et al., 2009) and in a variety of orogens globally (Clift, 2010). Our data show a temporal correlation with late Neogene climatic fluctuations; however, distribution is not sufficient to fully evaluate the role of climate on Alaska Range orogenesis. When we compare the global $\delta^{18}O$ compilation (Zachos et al., 2001) with plots of closure temperature versus age for different thermochronometers from the eastern Alaska Range, we see a temporal link between an increase in bedrock cooling rates on the north side of the Denali fault (based on the kink in slope at ~3 Ma) and the onset of Northern Hemisphere glaciation (Fig. 13; Lisiecki and Raymo, 2005; Zachos et al., 2001). Exhumation data from the south side of the Denali fault indicate a similar pattern, but at lower resolution, and with slower cooling and less rapid exhumation rates. This temporal correlation by no means proves that climate is forcing exhumation. However, the similarity in

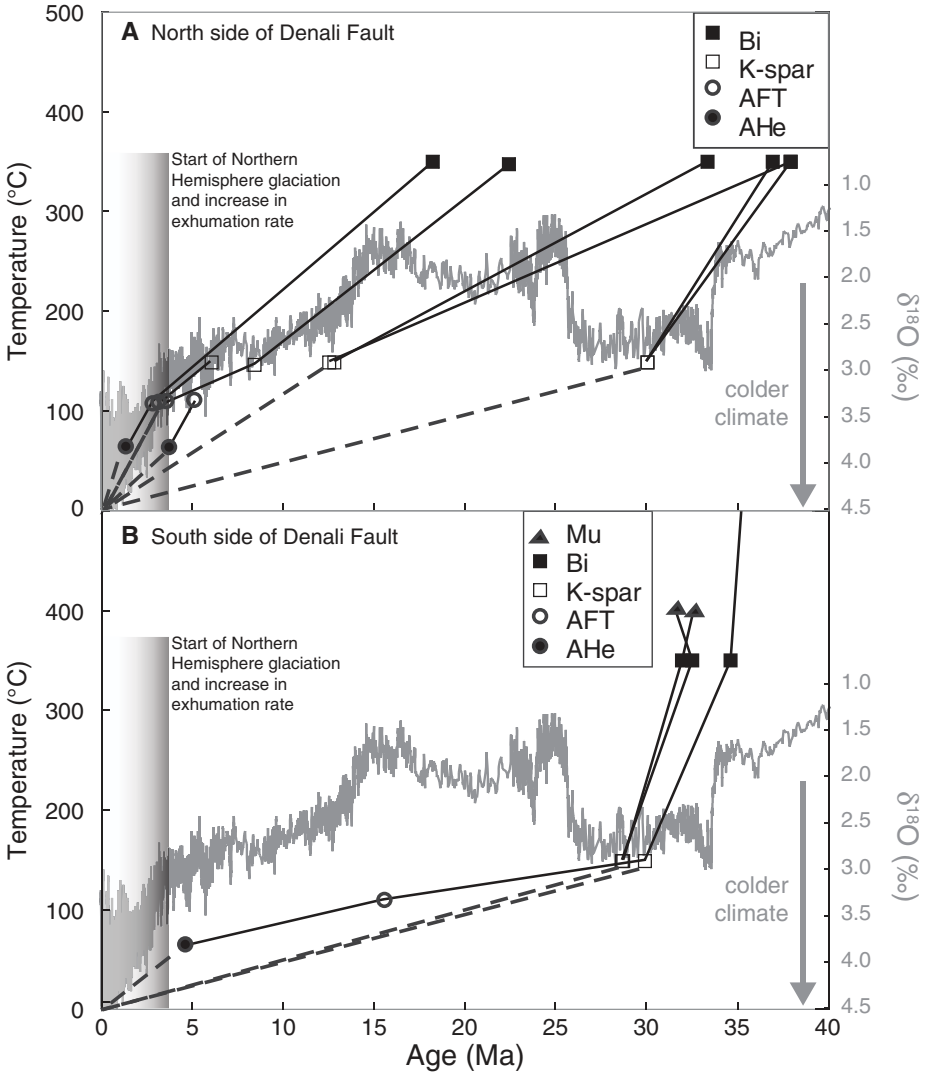


**Figure 13. Time-averaged temperature paths for individual samples from north (A) and south (B) of the Denali fault, based on multiple thermochronometers. Data include hornblende (550 °C; off graph), muscovite (Tc 400 °C; Mu) biotite (Tc 350 °C; Bi), K-spar (Tc 150 °C), AFT (Tc 110 °C), and AHE (Tc 65 °C) ages (Reiners and Ehlers, 2005). Samples with multiple cooling ages are shown. All samples are within ~10 km of the Denali fault. Cooling paths are assumed to be linear in between data points. $\delta^{18}O$ is modified from Zachos et al. (2001) and used as a proxy for world temperature trends. Samples north of the Denali fault show a marked increase in cooling rate at ~3 Ma. Limited data from samples south of the Denali fault show a marked increase in cooling rate at ~4–5 Ma.**

timing between climate change and exhumation in the eastern Alaska Range, combined with the vast number of other orogens showing similar linkages (Clift, 2010), suggests that climate may play a role in driving exhumation in the Alaskan interior.

A possible mechanism for a climate-related exhumation rate increase at ~3 Ma is the addition of glaciers in the Alaska Range (i.e., more efficient erosion processes [Hallet et al., 1996; Westgate et al., 1990]). It has been shown that glaciers and climatic instability in a tectonically active region have a greater effect on denudation processes than simple isostatic response to tectonic forces in a quasi-stable climate setting (Clift, 2010; Berger et al., 2008a; Berger et al., 2008b; Molnar and England, 1990). It has also been shown that periods of climatic instability where glaciers advance and retreat enhance erosion by allowing the erosive power of glaciers and the mass-transport capabilities of fluvial systems to work in tandem (Owen et al., 2008; Shuster et al., 2005; Zhang et al., 2001). The Alaska Range has a documented Pleistocene glacial history of numerous advance and retreat cycles (e.g., Briner and Kaufman, 2008).

In addition, a large percentage of the glaciers along the Denali fault system are rare surge-type glaciers (Echelmeyer et al., 1987; Post, 1969; St. Amand, 1957). Surge-type glaciers experience surge events, involving large increases in velocity and advancement at a fairly consistent recurrence interval of $10^2$ to $10^3$ years (Woodward et al., 2002; Raymond, 1987; Kamb et al., 1985) and present a unique case of glacier retreat and advance. Surge events are accompanied by an exponential increase in erosion relative to steady-state surge quiescence (Humphrey and Raymond, 1994; Smith, 1990). In light of recent work by Thomson et al. (2010), we feel it is important to point out that the subpolar eastern Alaska Range has modern glaciers with known high basal velocities. Thomson et al. (2010) demonstrate that low-velocity glacial cover can actually limit erosion rates. We make no claims on how long there have been surge-type glaciers along the Denali fault, but it is clear that high-velocity, surge-type glaciers have a definitive spatial correlation to the Denali fault system and not simply the region's current climatic regime (Manley and Daly, 2005; Raymond, 1987; Post, 1969). Based on our thermochronological analysis (Fig. 13), the Denali fault system may have experienced climate-induced Pliocene exhumation rate increases. Thus we postulate that the combination of lateral fault-strain accumulation with highly efficient, episodic surge-type and nonsurge glacial erosion contribute to high exhumation rates adjacent to the Denali fault during the late Cenozoic.

### Tectonic Driving Mechanisms of Neogene Exhumation in the Eastern Alaska Range

These new thermochronology data offer a long record of exhumation from the eastern Alaska Range. The first sign of rapid Neogene exhumation begins ~22 Ma and is consistent with early exhumation events in the western Alaska Range (~23 Ma; Haeussler et al., 2008). Our interpretation of the thermochronological data is consistent with the stratigraphic record of the Tanana basin, where Ridgway et al. (2007) interpret a transpressional foreland-basin system related to regional shortening of the Alaska Range, associated with strike-slip displacement along the Denali fault system. We also see the continuance of rapid exhumation from ~22 Ma to the present. The absence of a region-wide exhumation rate change in the eastern Alaska Range at ~6 Ma is curious considering the strong evidence that the central Alaska Range

(Mount McKinley region) and the western Alaska Range experienced a change in exhumation rate at ~6 Ma (Haeussler et al., 2008; Fitzgerald, et al., 1995). The central Alaska Range and western Alaska Range are located at the interface between the rotating southern Alaska block and the rotating Bering block (Cross and Freymueller, 2008; Fig. 1). The interactions between these tectonic entities likely have contributed to the complex patterns of exhumation occurring along the Alaska Range. More thermochronometric data with better spatial coverage across the entire Alaska Range will help constrain the near-field boundary conditions along the western Denali fault and test whether there are spatially and temporally complex exhumation patterns resulting from the interactions among these (micro) plates.

Our exhumation data from the Alaska Range correlate well with the initial timing of rapid Neogene exhumation in the eastern Chugach–St. Elias Mountains at ~20 Ma based on an AFT vertical profile on Mount Logan (~18 Ma; O'Sullivan and Currie, 1996) and a detrital zircon fission-track study on glacial outwash sands (Enkelmann et al., 2008, ~20 Ma). Additionally, the still active Wrangell volcanic field first developed ~23 Ma (Richter et al., 1990), suggesting that the early Miocene was an important time in the tectonic development of southern margin of Alaska.

The overall Neogene tectonic history of Alaska is not well constrained, but there is growing evidence from thermochronologic studies of exhumation events initiated at ~23 Ma, ~22 ma, ~20 Ma, ~16 Ma, ~11 Ma, ~6 Ma, 4 Ma, and ~1 Ma (Spotila and Berger, 2010; Berger et al., 2008a; Berger et al., 2008b; Haeussler et al., 2008; Enklemann et al., 2008; O'Sullivan and Currie, 1996; Fitzgerald et al., 1995; this study). In addition, strata in regional basins suggest pulses of enhanced exhumation occurred from the Miocene to present (Finzel et al., 2009; Haeussler et al., 2008; Ridgway et al., 2007; Lagoe et al., 1993). Though Alaska exhumation events since ~5 Ma have been correlated with climatic drivers by some researchers (e.g., Enkelmann et al., 2009; Berger et al. 2008a; Berger et al., 2008b), there is a general consensus that tectonic drivers have also been continual since the middle Miocene to present (e.g., Spotila and Berger, 2010).

The ~22 Ma initiation of rapid exhumation in the eastern Alaska Range is roughly correlative with the arrival of the Yakutat microplate into the southern Alaska subduction zone (Plafker et al., 1994). The Yakutat microplate is thought to dominantly consist of mafic oceanic plateau rocks (Plafker, 1987) between 15 and 35 km thick (Christeson et al., 2010; Eberhart-Phillips et al., 2006; Ferris et al., 2003). Although the timing of the arrival of the Yakutat microplate and the change from normal subduction to flat slab subduction and/or collision is poorly constrained, the longevity (~22 Ma to present) of rapid exhumation in the eastern Alaska Range and across south-central Alaska begs the question if the eastern Alaska Range long-term exhumation record is recording the timing of "collision" and the effects of continuing collision. This interpretation does not discount the influence of block rotation (Haeussler et al., 2008) or climatic influences on exhumation history (Berger et al., 2008a; Berger et al., 2008b). That said, both rotation of the southern Alaska block and quaternary tectonic/climate coupling are ultimately in the first order driven by tectonic processes at Alaska's southern margin subduction zone.

## CONCLUSIONS

We applied $^{40}Ar/^{39}Ar$ (hornblende, muscovite, biotite, and K-spar), AFT, and AHe thermochronology to examine the asymmetric topographic signature of the Denali fault in the eastern Alaska Range. We identified spatial variations in the amount of exhumation along and across strike and temporal variations in focus of exhumation. Rapid exhumation has been occurring since ~22 Ma with a zone of focused deep exhumation along, and on the north side, of the Denali fault. The youngest AFT ages (~1 Ma) were identified in the Nenana Mountain region where total Neogene exhumation is less than elsewhere in the region. We postulate a segment of the Denali fault has a north-dipping fault plane and the bend is fixed onto the south side of the Denali fault with the deforming edge currently in the Nenana Mountain region.

An exhumation rate increase in the Pliocene and Quaternary may be related to climate change. The coincident timing between exhumation and climate is most obviously expressed on the north side of the Denali fault, whereas the south side of the Denali fault indicates a more suppressed Pliocene–Quaternary increase in exhumation. This apparent Pliocene–Quaternary exhumation gradient across the fault could be due to a lack of data on the south side or a weaker tectonic forcing. Although we discussed a unique glacial-tectonic exhumation feedback loop for ice-covered, strike-slip faults, more information is needed to conclusively link increases in Pliocene–Quaternary exhumation rates to climate in the Alaska Range.

The longevity of rapid exhumation in the eastern Alaska Range demands a long-term driving mechanism. We suggest that by at least ~22 Ma, the Yakutat microplate was not undergoing standard subduction, but instead either flat-slab subduction or collision had initiated and continues today.

### ACKNOWLEDGMENTS

We would like to thank the Geological Society of America and the Geological Society of Alaska for supporting this research project through graduate research grants. We would also like to thank the American Alpine Club and Mugs Stump Climbing grant for field season funding. This manuscript benefited greatly from the constructive reviews of A. Berger, C. Sorlien, and S. Gulick. This research was also made possible by support from National Science Foundation grants EAR-0952793 and EAR-0952800. We thank W. Nokleberg for his work in the region and the numerous other Alaska-based research projects that were the foundation for this research. A special thanks to A. Sterns for field assistance.

### REFERENCES CITED

Aleinikoff, J.N., Farmer, G.L., Rye, R.O., and Nokleberg, W.J., 2000, Isotopic evidence for the sources of Cretaceous and Tertiary granitic rocks, east-central Alaska: Implications for the tectonic evolution of the Yukon-Tanana terrane: Canadian Journal of Earth Sciences, v. 37, p. 945–956, doi: 10.1139/cjes-37-6-945.

Bemis, S.P., and Wallace, W., 2007, Neotectonic framework of the north-central Alaska Range foothills, *in* Ridgway, K.D., Trop, J.M., Glen, J.M.G., and O'Neill, J.M., eds., Tectonic Growth of a Collisional Continental Margin: Crustal Evolution of Southern Alaska: Geological Society of America Special Paper 431, p. 549–572, doi: 10.1130/2007.2431(21).

Berger, A.L., Gulick, S.P.S., Spotila, J.A., Upton, P., Jaeger, J.M., Chapman, J.B., Worthington, L.A., Pavlis, T.L., Ridgway, K.D., Willems, B.A., and McAleer, R.J., 2008a, Quaternary tectonic response to intensified glacial erosion in an orogenic wedge: Nature Geoscience, v. 1, p. 793–799, doi: 10.1038/ngeo334.

Berger, A.L., Spotila, J.A., Chapman, J., Pavlis, T.L., Enkelmann, E., Ruppert, N.A., and Buscher, J.T., 2008b, Architecture, kinematics, and exhumation of a convergent orogenic wedge: A thermochronological investigation of tectonic-climatic interactions within the central St. Elias orogen, Alaska: Earth and Planetary Science Letters, v. 270, p. 13–24, doi: 10.1016/j.epsl.2008.02.034.

Braun, J., van der Beek, P., and Batt, G., 2006, Quantitative Thermochronology: Cambridge, Cambridge University Press.

Briner, J.P., and Kaufman, D.S., 2008, Late Pleistocene mountain glaciation in Alaska: Key chronologies: Journal of Quaternary Science, v. 23, p. 659–670, doi: 10.1002/jqs.1196.

Buscher, J.T., and Spotila, J.A., 2007, Near-field response to transpression along the southern San Andreas fault, based on exhumation of the northern San Gabriel Mountains, southern California: Tectonics, v. 26, p. TC5004, doi: 10.1029/2006TC002017.

Christeson, G.L., Gulick, S.P.S., van Avendonk, H.J.A., Worthington, L., Reece, R.S., and Pavlis, T.L., 2010, The Yakutat terrane: Dramatic change in crustal thickness across the Transition fault, Alaska: Geology, v. 38, p. 895–898, doi: 10.1130/G31170.1.

Clift, P.D., 2010, Enhanced global continental erosion and exhumation driven by Oligo-Miocene climate change: Geophysical Research Letters, v. 37, p. L09402, doi: 10.1029/2010GL043067.

Cormier, M.H., Seeber, L., McHugh, C.M.G., Polonia, A., Cagatay, N., Emre, O., Gasperini, L., Gorur, N., Bortoluzzi, G., Bonatti, E., Ryan, W.B.F., and Newman, K.R., 2006, North Anatolian fault in the Gulf of Izmit (Turkey): Rapid vertical motion in response to minor bends of a nonvertical continental transform: Journal of Geophysical Research, v. 111, B4, p. B04102, doi: 10.1029/2005JB003633.

Crone, A., Personius, S., Craw, P., Haeussler, P., and Staft, L., 2004, The Susitna Glacier thrust fault—Characteristics of ruptures that initiated the 2002 Denali fault earthquake: Bulletin of the Seismological Society of America, v. 94, no. 6B, p. S5–S22, doi: 10.1785/0120040619.

Cross, R., and Freymueller, J., 2008, Evidence for and implications of a Bering plate based on geodetic measurements from the Aleutians and western Alaska: Journal of Geophysical Research, v. 113, B07405, doi: 10.1029/2007JB005136.

Csejtey, B., Jr., Mullen, M.W., Cox, D.P., and Stricker, G.D., 1992, Geology and geochronology of the Healy quadrangle, south-central Alaska: U.S. Geological Survey Miscellaneous Investigations Map I-1961, scale 1:250,000.

Dair, L., and Cooke, M.L., 2009, San Andreas fault geometry through the San Gorgonio Pass, California: Geology, v. 37, p. 119–122, doi: 10.1130/G25101A.1.

Eberhart-Phillips, D., Haeussler, P.J., Freymueller, J.T., Frankel, A.D., Rubin, C.M., Craw, P., Ratchkovski, N.A., Anderson, G., Carver, G.A., Crone, A.J., Dawson, T.E., Fletcher, H., Hansen, R., Harp, E.L., Harris, R.A., Hill, D.P., Hreinsdottir, S., Jibson, R.W., Jones, L.M., Kayen, R.E., Keefer, D.K., Larsen, C.F., Moran, S.C., Personius, S.F., Plafker, G., Sherrod, B.L., Sieh, K., Sitar, N., and Wallace, W.K., 2003, The 2002 Denali fault earthquake, Alaska: A large magnitude slip-partitioned event: Science, v. 300, p. 1113–1118, doi: 10.1126/science.1082703.

Eberhart-Phillips, D., Christensen, D.H., Brocher, T.M., Hansen, R., Ruppert, N.A., Haeussler, P.J., and Abers, G.A., 2006, Imaging the transition from Aleutian subduction to Yakutat collision in central Alaska, with local earthquakes and active source data: Journal of Geophysical Research, v. 111, p. B11303, doi: 10.1029/2005JB004240.

Echelmeyer, K., Butterfield, R., and Cuillard, D., 1987, Some observations on a recent surge of Peters glacier, Alaska, U.S.A: Journal of Glaciology, v. 33, no. 115, p. 341–345.

Elliot, J.L., Larsen, C.F., Freymueller, J.T., and Motyka, R.J., 2010, Tectonic block motion and glacial isostatic adjustment in southeast Alaska and adjacent Canada constrained by GPS measurements: Journal of Geophysical Research, v. 115, doi: 10.1029/2009JB007139.

Enkelmann, E., Garver, J.I., and Pavlis, T.L., 2008, Rapid exhumation of ice-covered rocks of the Chugach–St. Elias orogen, Southeast Alaska: Geology, v. 36, no. 12, p. 915–918, doi: 10.1130/G2252A.1.

Enkelmann, E., Zeitler, P.K., Pavlis, T.L., Garver, J.I., and Ridgway, K.D., 2009, Intense localized rock uplift and erosion in the St. Elias orogen of Alaska: Nature Geoscience, v. 2, p. 360–363, doi: 10.1038/ngeo502.

Ferris, A., Abers, G.A., Christensen, D.H., and Veenstra, E., 2003, High resolution image of the subducted Pacific plate beneath central Alaska, 50–150 km depth: Earth and Planetary Science Letters, v. 214, no. 3–4, p. 575–588, doi: 10.1016/S0012-821X(03)00403-5.

Finzel, E., Ridgway, K., Reifenstuhl, R., Blodgett, R., White, J., and Decker, P., 2009, Stratigraphic framework and estuarine depositional environments of the Miocene Bear Lake Formation, Bristol Bay Basin, Alaska: Onshore equivalents to potential reservoir strata in a frontier gas-rich basin: American Association of Petroleum Geologists Bulletin, v. 93, no. 3, p. 379–405, doi: 10.1306/10010808030.

Fisher, M.A., Ratchkovski, N.A., Nokleberg, W.J., Pellerin, L., and Glen, J.M.G., 2004, Geophysical data reveal the crustal structure of the Alaska Range orogen within the aftershock zone of the Mw 7.9 Denali fault earthquake: Bulletin of the Seismological Society of America, v. 94, p. S107–S131, doi: 10.1785/0120040613.

Fitzgerald, P.G., Stump, E., and Redfield, T.F., 1993, Late Cenozoic uplift of Denali and its relation to relative plate motion and fault morphology: Science, v. 259, p. 497–499.

Fitzgerald, P.G., Sorkhabi, R., Redfield, T., and Stump, E., 1995, Uplift and denudation of the central Alaska Range: A case study in the use of apatite fission-track thermochronology to determine absolute uplift parameters: Journal of Geophysical Research, v. 100, p. 20,175–20,191, doi: 10.1029/95JB02150.

Haeussler, P.J., 2008, An overview of the neotectonics of interior Alaska, far-field deformation from the Yakutat Microplate collision: Geophysical Monograph, v. 179, p. 83–108.

Haeussler, P.J., Bruhn, R.L., and Pratt, T.L., 2000, Potential seismic hazards and tectonics of the upper Cook Inlet basin, Alaska, based on analysis of Pliocene and younger deformation: Geological Society of America Bulletin, v. 112, p. 1414–1429.

Haeussler, P.J., Schwartz, D.P., Dawson, T.E., Stenner, H.D., Lienkaemper, J.J., Cinti, F., Montone, P., Sherrod, B., and Craw, P., 2004, Surface rupture of the 2002 Denali Fault, Alaska, Earthquake and comparison with other strike-slip ruptures: Earthquake Spectra, v. 20, p. 565–578.

Haeussler, P.J., O'Sullivan, P., Berger, A.L., and Spotila, J.A., 2008, Neogene exhumation of the Tordrillo Mountains, Alaska, and correlations with Denali (Mt. McKinley), *in* Freymueller, J.J., Haeussler, P.J., Wesson, R., and Ekstrom, G., Active Tectonics and Seismic Potential of Alaska: Washington, D.C., American Geophysical Union Monograph 179, p. 269–285.

Hallet, B., Hunter, L., and Bogen, J., 1996, Rates of erosion and sediment evacuation by glaciers: A review of field data and their implications: Global and Planetary Change, v. 12, p. 213–235, doi: 10.1016/0921-8181(95)00021-6.

Harrison, T.M., Celerier, J., Aikman, A.B., Hermann, J., and Heizler, M.T., 2009, Diffusion of $^{40}$Ar in muscovite: Geochimica et Cosmochimica Acta, v. 73, p. 1039–1051, doi: 10.1016/j.gca.2008.09.038.

Harrison, W.D., and Post, A., 2003, How much do we really know about glacier surges?: Annals of Glaciology, v. 36, p. 1–6, doi: 10.3189/172756403781816185.

Hilley, G., and Arrowsmith, J., 2008, Geomorphic response to uplift along the Dragon's Back pressure ridge, Carrizo Plain: California Geology, v. 36, doi: 10.1130/G24517A.1.

Humphrey, N.F., and Raymond, C.F., 1994, Hydrology, erosion and sediment production in a surging glacier: Variegated glacier, Alaska, 1982–1983: Journal of Glaciology, v. 40, no. 136, p. 539–552.

Kamb, B., Raymond, C., Harrison, W., Engelhardt, H., Echelmeyer, K., Humphrey, N., Brugman, M., and Pfeffer, T., 1985, Glacier surge mechanism: 1982–1983 surge of Variegated glacier, Alaska: Science, v. 227, p. 469–479, doi: 10.1126/science.227.4686.469.

Lagoe, M.B., Eyles, C.H., Eyles, N., and Hale, C., 1993, Timing of late Cenozoic tidewater glaciation in the far North Pacific: Geological Society of America Bulletin, v. 105, p. 1542–1560, doi: 10.1130/0016-7606.

Lisiecki, L.E., and Raymo, M.E., 2005, A Pliocene–Pleistocene stack of 57 globally distributed benthic $\delta^{18}$O records: Paleoceanography, v. 20, p. PA1003, doi: 10.1029/2004PA001071.

Little, T.A., Cox, S., Vry, J.K., and Batt, G., 2005, Variations in exhumation level and uplift rate along the oblique-slip Alpine fault, central Southern Alps, New Zealand: Geological Society of America Bulletin, v. 117, p. 707–723, doi: 10.1130/B25500.1.

Lovera, O., Grove, M., and Harrison, T., 2002, Systematic analysis of K-feldspar $^{40}$Ar/$^{39}$Ar step-heating results II: Relevance of laboratory argon diffusion properties to nature: Geochimica et Cosmochimica Acta, v. 66, no. 7, p. 1237–1255, doi: 10.1016/S0016-7037(01)00846-8.

Lu, Z., Wright, T., and Wicks, C., 2003, Deformation of the 2002 Denali fault earthquakes mapped by Radarsat-1 interferometry: Eos (Transactions, American Geophysical Union), v. 84, no. 41, doi: 10.1029/2003EO410002.

Manley, W.F., and Daly, C., 2005, Alaska geospatial climate animations of monthly temperature and precipitation: Institute of Arctic and Alpine Research, University of Colorado, http://instaar.colorado.edu/QGISL/AGCA.

Matmon, A., Schwartz, D., Haeussler, P., Finkel, R., Lienkaemper, J., Stenner, H., and Dawson, T., 2006, Denali fault slip rates and Holocene–late Pleistocene kinematics of central Alaska: Geology, v. 34, no. 8, p. 645–648, doi: 10.1130/G22361.1.

McAleer, R., Spotila, J., Enkelmann, E., and Berger, A., 2009, Exhumation along the Fairweather fault, southeastern Alaska, based on low-temperature thermochronometry: Tectonics, v. 28, p. TC1007, doi: 10.1029/2007TC002240.

McDougall, I., and Harrison, T.M., 1999, Geochronology and Thermochronology by the $^{40}$Ar/$^{39}$Ar Method (2nd edition): New York, Oxford University Press, 269 p.

Mériaux, A.-S., Sieh, K., Finkel, R.C., Rubin, C.M., Taylor, M.H., Meltzner, A.J., and Ryerson, F.J., 2009, Kinematic behavior of southern Alaska constrained by westward decreasing postglacial slip rates on the Denali fault, Alaska: Journal of Geophysical Research, v. 114, p. B03404, doi: 10.1029/2007JB005053.

Molnar, P., and England, P., 1990, Late Cenozoic uplift of mountain ranges and global climate change: Chicken or egg?: Nature, v. 346, p. 29–34, doi: 10.1038/346029a0.

Nokleberg, W.J., Aleinikoff, J.N., Dutro, J.T., Jr., Lanphere, M.A., Silberling, N.J., Silva, S.R., Smith, T.E., and Turner, D.L., 1992, Map, tables, and summary of fossil and isotopic age data, Mount Hayes quadrangle, eastern Alaska Range, Alaska: U.S. Geological Survey Miscellaneous Field Studies Map 1996-D, scale 1:250,000.

O'Sullivan, P., and Currie, L., 1996, Thermotectonic history of Mt. Logan, Yukon Territory, Canada: Implications of multiple episodes of middle to late Cenozoic denudation: Earth and Planetary Science Letters, v. 144, p. 251–261, doi: 10.1016/0012-821X(96)00161-6.

Owen, L.A., Thackray, G., Anderson, R.S., Briner, J.P., Kaufman, D., Roe, G., Pfeffer, W., and Yi, C., 2008, Integrated mountain glacier research: Current status, priorities, and future prospects: Geomorphology, v. 103, p. 158–171, doi: 10.1016/j.geomorph.2008.04.019.

Plafker, G., 1987, Regional geology and petroleum potential of the northern Gulf of Alaska continental margin, *in* Scholl, D.W., et al., eds., Geology and Resource Potential of the Continental Margin of Western North America and Adjacent Ocean Basins: Circum-Pacific Council for Energy and Mineral Resources Earth Science Series, v. 6, p. 229–268.

Plafker, G., Naeser, C.W., Zimmermann, R.A., Lull, J.S., and Hudson, T., 1992, Cenozoic uplift history of the Mount McKinley area in the central Alaska Range based on fission-track dating: U.S. Geological Survey Bulletin 2041, p. 202–212.

Plafker, G., Moore, J.C., and Winkler, G.R., 1994, Geology of the southern Alaska margin, *in* Plafker, G., and Berg, H.C., eds., The Geology of Alaska: Boulder, Colorado, Geological Society of America, Geology of North America, v. G-1, p. 389–449.

Post, A., 1969, Distribution of surging glaciers in western North America: Journal of Glaciology, v. 8, p. 229–240.

Ratchkovski, N.A., Wiemer, S., and Hansen, R.A., 2004, Seismotectonics of the Central Denalis Fault, Alaska, and the 2002 Denali Fault Earthquake Sequence: Bulletin of the Seismological Society of America, v. 94, p. S156–S174, doi:10.1785/0120040621.

Raymond, C.F., 1987, How do glaciers surge?: A review: Journal of Geophysical Research, v. 92, no. B9, p. 9121–9134, doi: 10.1029/JB092iB09p09121.

Reiners, P.W., and Ehlers, T.A., eds., 2005, Low-Temperature Thermochronology: Techniques, Interpretations, Applications, Volume 58: Reviews in Mineralogy and Geochemistry: Chantilly, Virginia, Mineralogical Society of America, Geochemical Society, 622 p.

Richter, D.H., Smith, J.B., Lanphere, M.A., Dalrymple, G.B., Reed, B.L., and Shew, N., 1990, Age and progression of volcanism, Wrangell volcanic field, Alaska: Bulletin of Volcanology, v. 53, p. 29–44.

Ridgway, K., Thoms, E., Layer, P., Lesh, M., White, J., and Smith, S., 2007, Neogene transpressional foreland basin development on the north side of the central Alaska Range, Usibelli Group and Nenana Gravel, Tanana basin, *in* Ridgway, K.D., et al., Tectonic Growth of a Collisional Continental Margin: Crustal Evolution of Southern Alaska: Geological Society of America Special Paper 431, p. 507–547, doi: 10.1130/2007.2431(20).

Roeske, S., Till, A., Foster, D., and Sample, J., 2007, Introduction, *in* Till, A., Roeske, S., Foster, D., and Sample, J., eds., Uplift and Extension along Continental Strike-Slip Faults: Geological Society of America Special Paper 434, p. 15–33.

Sherwood, K.L., and Craddock, C., 1979, General geology of the central Alaska Range between the Nenana River and Mount Deborah: Alaska Division of Geological and Geophysical Surveys Open-File Report AOF-116, scale 1:63,360, 3 sheets.

Shuster, D.L., Ehlers, T.A., Rusmore, M.E., and Farley, K.A., 2005, Rapid glacial erosion at 1.8 Ma revealed by $^{4}He/^{3}He$ thermochronometry: Science, v. 310, p. 1668–1670, doi: 10.1126/science.1118519.

Smith, N.D., 1990, The effects of glacial surging on sedimentation in a modern ice-contact lake, Alaska: Geological Society of America Bulletin, v. 102, p. 1393–1403, doi: 10.1130/0016-7606(1990)102<1393:TEOGSO>2.3.CO;2.

Spotila, J., and Berger, A., 2010, Exhumation at orogenic indentor corners under long-term glacial conditions: Example of the St. Elias orogen, southern Alaska: Tectonophysics, v. 490, p. 241–256, doi: 10.1016/j.tecto.2010.05.015.

Spotila, J.A., Farley, K.A., and Sieh, K., 1998, Uplift and erosion of the San Bernardino Mountains associated with transpression along the San Andreas fault, California, as constrained by radiogenic helium thermochronology: Tectonics, v. 17, p. 360–378, doi: 10.1029/98TC00378.

Spotila, J.A., Niemi, N., Brady, R., House, M., and Buscher, J., 2007, Long-term continental deformation associated with transpressive plate motion: The San Andreas fault: Geology, v. 35, p. 967–970, doi: 10.1130/G23816A.1.

St. Amand, P., 1957, Geological and geophysical synthesis of the tectonics of portions of British Columbia, the Yukon Territory, and Alaska: Geological Society of America Bulletin, v. 68, p. 1343–1370, doi: 10.1130/0016-7606(1957)68[1343:GAGSOT]2.0.CO;2.

Sylvester, A.G., 1988, Strike-slip faults: Geological Society of America Bulletin, v. 100, p. 1666–1703, doi: 10.1130/0016-7606(1988)100<1666:SSF>2.3.CO;2.

Thomson, S.N., Brandon, M.T., Tomkin, J.H., Reiners, P.W., Vasquez, C., and Wilson, N.J., 2010, Glaciation as a destructive and constructive control on mountain building: Nature, v. 467, p. 313–317.

Wahrhaftig, C., Turner, D., Weber, F., and Smith, T., 1975, Nature and timing of movement on Hines Creek strand of Denali fault system, Alaska: Geology, v. 3, no. 8, p. 463–466, doi: 10.1130/0091-7613(1975)3<463:NATOMO>2.0.CO;2.

Westgate, J.A., Stemper, B.A., and Pewe, T.L., 1990, A 3 m.y. record of Pliocene–Pleistocene loess in interior Alaska: Geology, v. 18, p. 858–861, doi: 10.1130/0091-7613(1990)018<0858:AMYROP>2.3.CO;2.

Whipple, K., 2009, The influence of climate on the tectonic evolution of mountain belts: Nature Geoscience, v. 2, p. 97–104, doi: 10.1038/ngeo413.

Woodward, J., Carver, S., Kunzendorf, H., and Bennike, O., 2002, Observations of surge periodicity in East Greenland using molybdenum records from marine sediment cores, *in* Dowdeswell, J.A., and Ó Cofaigh, C., eds., Glacier-Influenced Sedimentation on High-Latitude Continental Margins: The Geological Society of London Special Publication 203, p. 367–373.

Zachos, J., Pagani, M., Sloan, L., Thomas, E., and Billups, K., 2001, Trends, rhythms, and aberrations in global climate 65 Ma to present: Science, v. 292, p. 686–693, doi: 10.1126/science.1059412.

Zhang, P.Z., Molnar, P., and Downs, W.R., 2001, Increased sedimentation rates and grain sizes 2–4 Myr ago due to the influence of climate change on erosion rates: Nature, v. 410, p. 891–897, doi: 10.1038/35073504.

Manuscript Received 11 February 2010
Revised Manuscript Received 23 September 2010
Manuscript Accepted 17 October 2010